EXPERIMENTAL STUDY ON A CROSS FLOW PLATE-TYPE DEHUMIDIFIER FOR A LIQUID DESICCANT COOLING SYSTEM

Mustafa Jaradat, Roland Heinzen, Ulrike Jordan, Klaus Vajen

Institute for Thermal Engineering, Kassel University, Kurt-Wolters-Str. 3, 34125-Kassel, Germany
Phone: + 49 561 804 3890, Fax: + 49 561 804 3993, www.solar.uni-kassel.de, solar@uni-kassel.de

Abstract

A cross-flow plate-type heat and mass exchanger is developed and experimentally examined as a dehumidifier in a liquid desiccant system. The sorbent used is lithium chloride (LiCl). The dehumidifier utilizes novel components and ideas in order to overcome the present obstacles such as the carryover of the sorbent into the air stream and the flow maldistribution of the sorbent over the exposed surfaces.

First experimental results show fairly effective air dehumidification. The dehumidifier was investigated without internal cooling of the sorbent. The performance of the dehumidifier was characterized by the moisture removal rate and dehumidification efficiency. The influence of the supply air flow rate, inlet temperature and relative humidity, and the desiccant flow rate on the performance was investigated.

During the measurements the relative humidity of the incoming air was decreased by about $\Delta\varphi = 13 \ to \ 41$ points, corresponding to a drop of the absolute humidity of $\Delta\omega = 1.5 \ to \ 4.8$ g/kg, while the air temperature increased in the range of $\Delta T = 3 \ to \ 6$ K. The respective moisture removal rate and the dehumidifier effectiveness were evaluated

1. Introduction

The main thermodynamic disadvantage of vapor-compression air-conditioning systems is the inefficient dehumidification process. The handling of the latent load requires cooling of the air below its dew point resulting in a lower air temperature than needed. Beyond, additional energy is needed to reheat the air to the required temperature. Liquid desiccant air-conditioning systems remove the latent load directly from the air by absorbing the moisture using a hygroscopic salt solution e.g. LiCl or calcium chloride ($CaCl_2$).

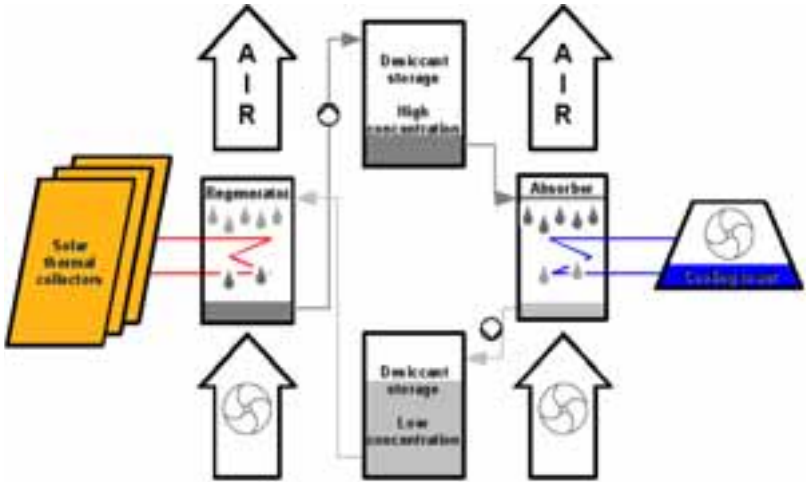

Fig. 1. Schematic diagram of a solar driven liquid desiccant air-conditioning system [1]

The main components of an open-loop liquid desiccant air-conditioning system are the dehumidifier (absorber) and the regenerator (desorber), as shown in Fig. 1. In the absorber, moisture which is absorbed from the conditioned air stream dilutes the desiccant solution. The diluted solution is reconcentrated in the regenerator, where it is heated to elevate its water vapor pressure. A scavenging air stream contacts the heated solution in the regenerator. There, water evaporates from the desiccant solution into the air and the solution is reconcentrated.

In the 1930's Kathabar Inc. [2] already produced a LiCl system, primarily for industrial applications. Despite the intensive research that has been conducted to develop these systems, there are still disadvantages of packed bed structures in absorbers and regenerators, like high pressure drop, high auxiliary energy consumption, high liquid to air ratio, flooding risks and the entrainment of desiccant mists into the air stream.

Recent studies [3-5] have shown that it is possible to reduce the desiccant flow rate essentially and to prevent carry-over by using a parallel plate structure to obtain regular cross-sections for the air flow. For this design, the need for a sophisticated fluid distribution system emerges as the low desiccant flow rate needs to be equally distributed over a fairly large area.

2. Description of the investigated dehumidifier

In the heat and mass exchanger prototype, the desiccant solution and the air stream are brought into contact in a cross flow configuration. The dehumidifier consists of a stack of plates, made of standard twin wall polycarbonate (PC). Each plate has a surface area of 600 x 600 mm^2 and a thickness of 6 mm. The inner chambers of the twin wall plates are used for the internal water driven cooling-circuit. The plates are covered with a promising fleece fiber in order to increase the exposure time of the desiccant on the plates and thereby enhance the desired mass transfer and heat exchange. The fleece thickness is 0.5 mm and it was tested regarding the absorption capacity and the diffusion behavior of the desiccant solution [6]. The overall exposed surface area of the investigated absorber is about 3.9 m^2. Fig. 2 shows the dehumidifier.

The dehumidifier was insulated with 25mm thick double layer of synthetic rubber Armaflex® with a thermal conductivity of $\lambda = 0.033$ W/m.K. The front side of the dehumidifier was insulated with removable extruded polystyrene foam sheet ($\lambda = 0.08$ W/m.K) for better visibility.

Fig. 2. The dehumidifier in the pilot plant stage, laboratories of Kassel University (August 2009)

The distribution system of the sorbent uses parallel plexiglass tubes to horizontally distribute the LiCl solution over the fleece. The tubes penetrate the dehumidifier stack of plates horizontally and spread the desiccant solution over the coated plates through a number of equally spaced holes.

The size and number of the holes are selected according to distribution tests carried out [6] to provide the desired liquid flow.
Therewith, the dehumidifier design is aimed at

- uniform distribution of the desiccant solution at different flow rates
- stability against corrosion induced by the desiccant solution
- using inexpensive and commercially available materials.

3. Instrumentation and experimental setup

The schematic of the experimental setup is shown in Fig. 3. Supply air and desiccant solution flow the heat and mass exchanger in a cross flow configuration. The air handling system consists of a heating coil, a humidifier and a radial blower. The liquid desiccant system consists of two solution tanks and solution pump. A lithium chloride aqueous solution is used as the desiccant in the system.
The desiccant strong solution is prepared with a 43% LiCl mass fraction ($\boldsymbol{\xi_{des.,in}}$). Throughout the tests the solution is re-concentrated by adding salt to the weak one.

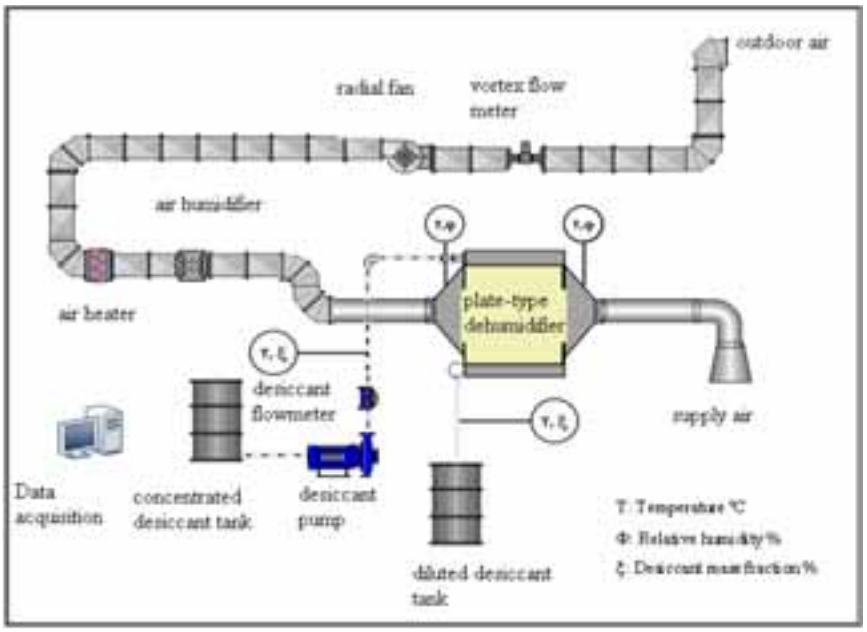

Fig. 3 Schematic diagram of the experimental setup

The concentrated hygroscopic salt solution is supplied to the dehumidifier from a plastic storage tank. It is diluted in the absorption process and pumped to a second tank.
The flow rate of the strong LiCl solution is continually monitored by using a magneto-inductive flow meter. The solution passes through a filter with a pore size of 300 μm in order to remove any contaminants that might affect the discharge bores along the Plexiglas pipes. The weak LiCl solution concentration is continuously monitored by a density transmitter.
The inlet and outlet of the dehumidifier are connected to a 250 mm-diameter flexible duct. The inlet and outlet temperatures and relative humidity of the air are measured with a combined capacitive humidity sensor and a PT100 sensor for temperature. The air volume flow rate through the air duct system can vary from 380-1800 m^3/h. The air duct system is equipped with a steam generator (10 kg/h) and an electrical heater (40 kW) in order to set the relative humidity of the supply air according to desired conditions. A summary of the technical data regarding the air and desiccant circuits is shown in Tables 1 and 2, respectively.

Table 1: The technical data of the sensors used in air flow detection

	Temperature	Relative humidity	Flowmeter
Principle	Pt100 1/3 DIN	Hygromer AC-1	Vortex flowmeter
Manufacturer	Rotronic	Rotronic	KROHNE
Model	HygroClip S	HygroClip S	Optiswirl 4070 c
Measurement Range	– 40°C - 80°C	0% -100% RH	159.62 – 2128.27 m3/h
Uncertainty	± 0.3 °C	± 1 %	± 2 %

Table 2: The technical data of the sensors used in desiccant flow detection

	Temperature	Concentration	Flowmeter
Principle	Pt1000	Digital refractometer	Magnetic Inductive
Manufacturer	Greisinger Electronic	ATAGO Co., LTD.	Endress+hauser
Model	GTH 175 / Pt	PAL-RI	FlowTec Picomag DMI 6530
Measurement Range	-199.9 ... +199.9°C	RI *1.3306 - 1.5284	0-100 l/h
Uncertainty	±0.1%	RI ±0.0003	± 0.5%

*RI: Refractometer Index

4. Measurements

Thirteen measurements were carried out with duration of about 45 minutes each, to reach quasi-steady state conditions. The experiments were conducted by varying one of the inlet parameters of the air and the desiccant that influence the dehumidifier performance. During dehumidification the air relative humidity is reduced while the air temperature increased. During the measurements the relative humidity of the incoming air was decreased by about $\Delta\varphi = 13 \; to \; 41 \, points$, corresponding to an drop of the absolute humidity of $\Delta\omega = 1.5 \; to \; 4.8 \, g/kg$, while the air temperature increased in the range of $\Delta T = 3 \; to \; 6 \, K$. In the measurement shown in Fig. 4, the air relative humidity decreased by about 32 points and the air temperature increased by about 5.5 K for quasi-steady state conditions.

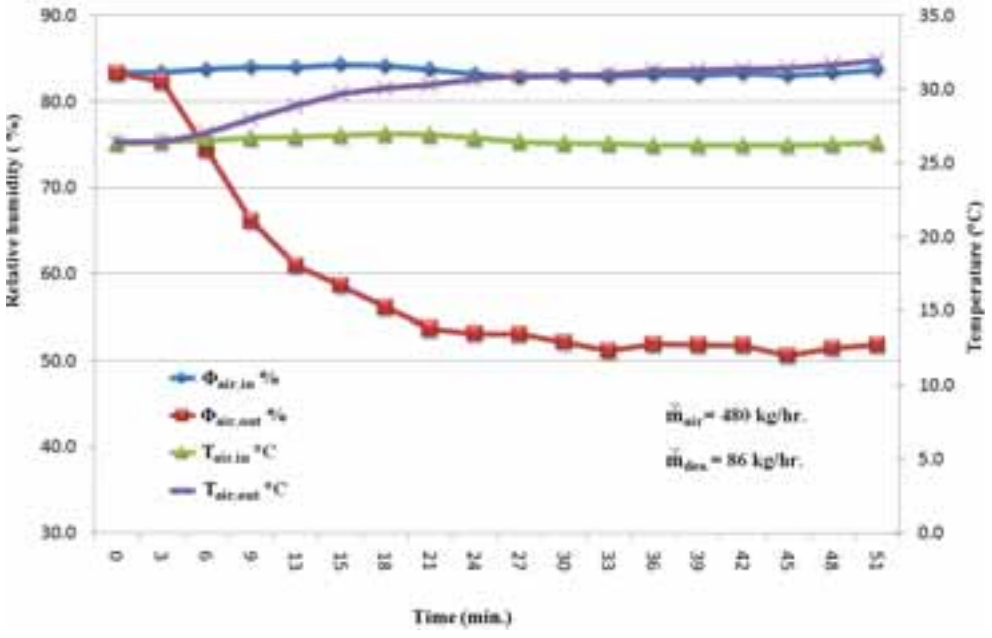

Fig. 4 The interaction between the inlet parameters in one of the experimental runs.

4.1 Parameters variations

Four test sequences were carried out by varying one of the inlet parameters, i.e. the desiccant or air flow rate, the air inlet temperature or humidity ratio. Table 3 summarizes the inlet parameters.

In the test sequences 1 to 4 the desiccant flow rate ($\dot{\mathbf{m}}_{\mathbf{des.}}$), the inlet air absolute humidity ($\boldsymbol{\omega}_{\mathbf{air,in}}$), the air flow rate ($\dot{\mathbf{m}}_{\mathbf{air}}$), and the air inlet temperature ($\mathbf{T}_{\mathbf{air,in}}$) were varied, respectively, while the remaining inlet parameters were set to nearly equal values for each of the measurements. The deviations of these inlet parameters from the set values shown in Table 3 are due to measurement constraints. Thus, the intervals given (e.g. $\overline{\mathbf{T}}_{\mathbf{air,in}}$ ± x) are not uncertainties of the measurements but they show the variations of measured input values.

Table 3: Summary of the experimental sets, and the operation conditions regarding the air and the desiccant. The shadowed cells show the parameter varied during the test sequence.

	$\overline{\mathbf{T}}_{\mathbf{air,in}}$ °C	$\overline{\boldsymbol{\omega}}_{\mathbf{air,in}}$ g/kg	$\overline{\dot{\mathbf{m}}}_{\mathbf{air}}$ kg/h	$\overline{\dot{\mathbf{m}}}_{\mathbf{des.}}$ kg/h
Test seq. 1	26 ± 0.2	20 ± 0.5	460 ± 8.0	var: 19.3 to 96.6
Test seq. 2	25.4 ± 0.6	var: 13.6 to 18.6	478 ± 10.0	98.3 ± 2
Test seq. 3	25.8 ± 0.8	17.6 ± 1.0	var: 480 to 728	84.3 ± 1.5
Test seq. 4	var: 25.2 to 33.2	19.1 ± 0.4	470 ± 7.0	98.2 ± 1.2

4.2 Moisture removal rate and dehumidification efficiency

The mass transfer performance of the dehumidifier was evaluated in terms of the moisture removal rate, $\dot{m}_v$ and the dehumidifier efficiency, ε.

The moisture removal rate is defined as

$$\dot{m}_v = \dot{m}_a \cdot (\omega_{a,in} - \omega_{a,out}) \quad (1)$$

where $\dot{m}_a$ is air mass flow rate (kg/s), $\omega_{a,in}$ and $\omega_{a,out}$ are the inlet and outlet air humidity ratio (g/kg), respectively.

The dehumidification efficiency of the absorber unit is defined as:

$$\varepsilon = \frac{\omega_{a,in} - \omega_{a,out}}{\omega_{a,in} - \omega_{e,in}} \quad (2)$$

where $\omega_{e,in}$ is the equilibrium humidity ratio at the inlet desiccant solution temperature and concentration. It would be obtained when the partial pressure of water in the air is equal to the vapor pressure of the inlet desiccant solution, i.e. when the driving force for mass transfer is zero. And it is given by:

$$\omega_e = 0.6198 \cdot \frac{p_s}{p_{atm.} - p_s} \quad (3)$$

where P_s is the saturation pressure in (kPa) and is calculated by Eq. 4, which has been derived from Othmer chart that describes the relation between the vapor pressure against the lithium chloride solution temperature [7].

$$p_s(T) = 3 \cdot 10^{-9} T_{des.,in}^5 - 4 \cdot 10^{-7} T_{des.,in}^4 + 3 \cdot 10^{-5} T_{des.,in}^3 + 2 \cdot 10^{-4} T_{des.,in}^2 - 0.0126 T_{des.,in} + 0.3 \quad (4)$$

In the following, influence of the desiccant and air flow rates, the air inlet temperature and humidity ratio on the outlet parameters are analyzed.

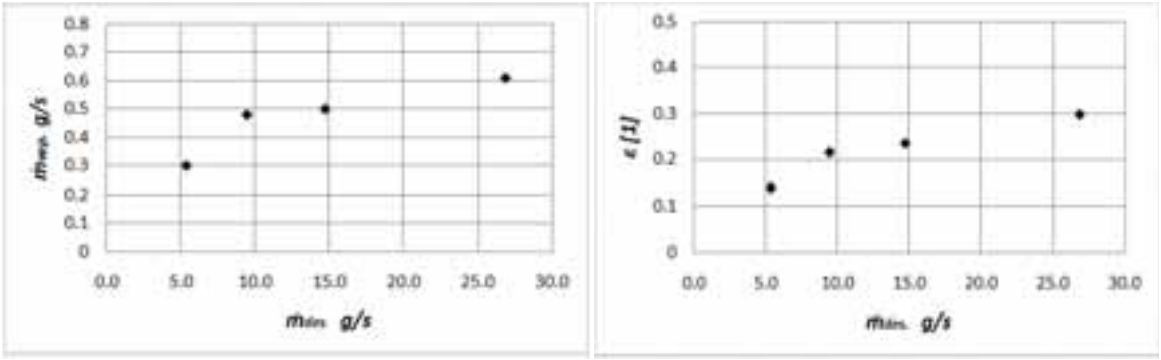

Fig. 5. Test sequence 1: Moisture removal rate and dehumidification efficiency over the desiccant mass flow rate.

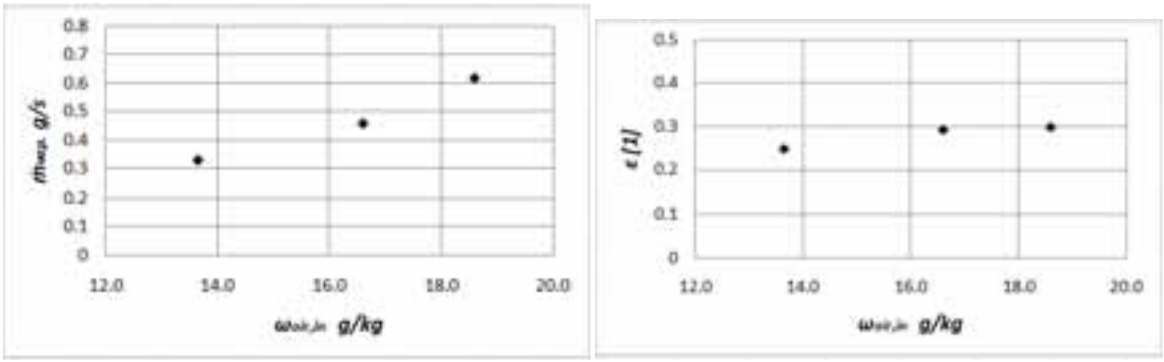

Fig. 6. Test sequence 2: Moisture removal rate and dehumidification efficiency over the absolute humidity of the inlet air.

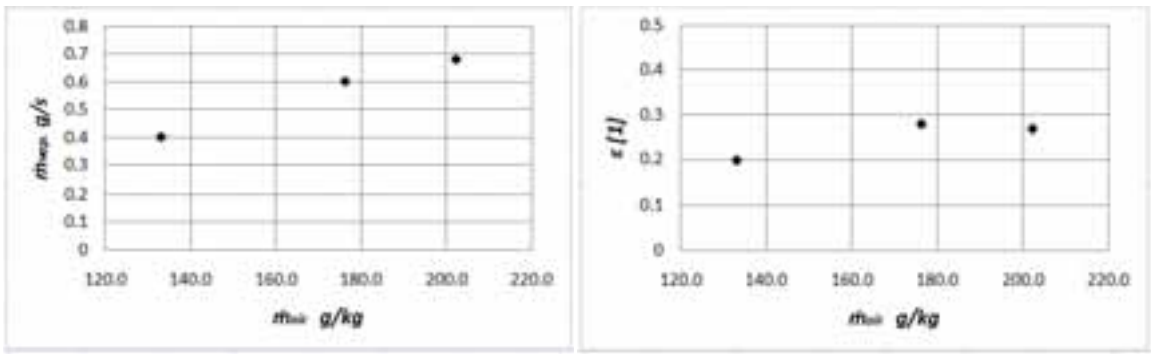

Fig. 7. Test sequence 3: Moisture removal rate and dehumidification efficiency over the air flow rate.

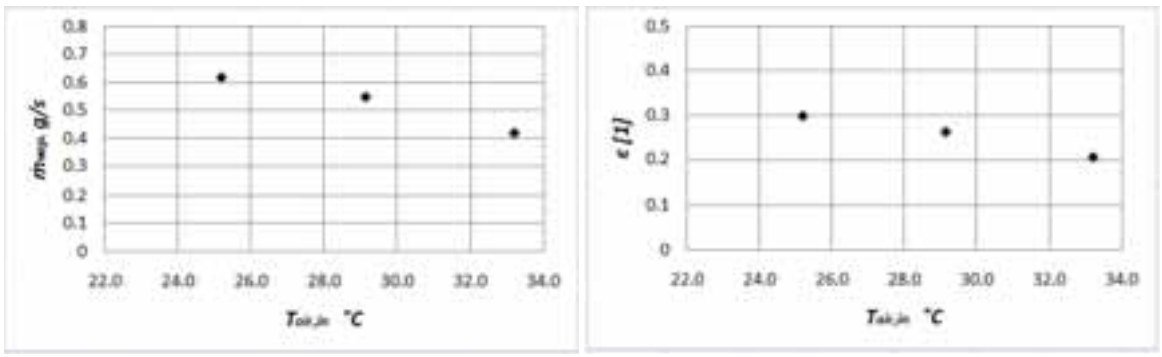

Fig. 8. Test sequence 4: Moisture removal rate and dehumidification efficiency over the air inlet temperature.

4.2.1 Desiccant flow rate

In the first test sequence, the effect of desiccant flow rate on the moisture removal rate and dehumidification efficiency is investigated. As shown in Fig. 5, both the moisture removal rate and the dehumidification efficiency increase remarkably with increasing desiccant flow rate. This is due to the decrease of the water vapor pressure at the surface of the desiccant with increasing flow rates, leading to an increase of the driving water vapor pressure difference between the desiccant and the air, i.e. reduction in the supply air humidity ratio as shown in Figure 9.

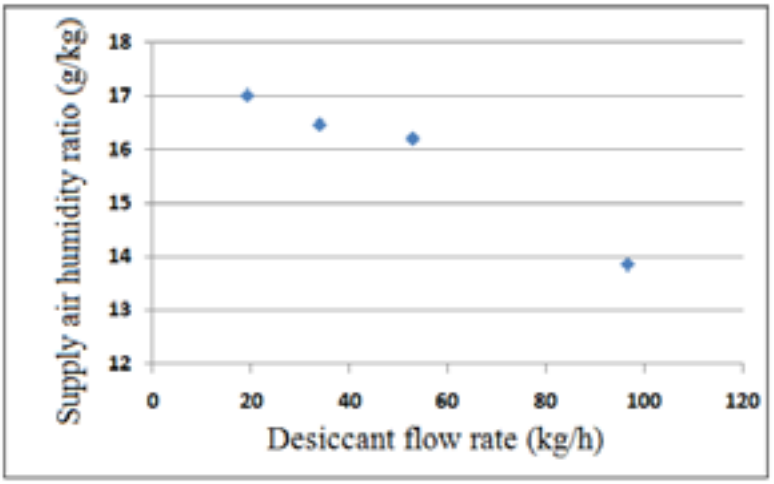

Fig. 9. Supply air humidity ratio over the desiccant flow rate for test sequence 1

4.2.2 Air absolute humidity

Fig. 6 shows the moisture removal rate and dehumidification efficiency over the absolute humidity of the inlet air as measured in test sequence 2. Evidently, the higher the absolute humidity of the inlet air, the higher the water vapor pressure difference between the air and the desiccant and therefore, the higher the moisture removal rate. On the other hand, the dehumidification efficiency is nearly constant since an increasing air inlet humidity ratio will increase both, the numerator and denominator of Eq.2.

4.2.3 Air flow rate

Similar to the curves shown in Fig. 6, Fig. 7 shows a sharp increase of the moisture removal rate, while the dehumidification efficiency is almost unchanged with increasing air flow rate (test sequence 3). In the same way, due to a higher air flow rate, the vapor pressure difference between the desiccant and the air and therewith the moisture removal rate is increased, while a higher air flow rate reduces both, the outlet and the equilibrium air humidity ratios in Eq. 2.

4.2.4 Air inlet temperature

Fig. 8 shows the moisture removal rate and dehumidification efficiency over the air inlet temperature as measured in test sequence 4. The higher the air inlet temperature, the higher the desiccant temperature, due to sensible heat transfer from the air to the desiccant, and the higher the vapor pressure at the desiccant surface. This reduces the moisture removal rate as well as the dehumidification efficiency.

5. Conclusions

The experimental results of supply air dehumidification provide effective air dehumidification. The reduction in the supply air humidity ratio ($\Delta\omega_{mean}$) could reach 4.8 g/kg, and a storage capacity *(SC)* that could reach about 440 KJ/m^3.

The paper experimentally studied the mass transfer between the air and the desiccant when they cross flow through a plate-type dehumidifier. The moisture removal rate and dehumidification efficiency characterize the mass transfer process. The measurements show an increase of the moisture removal rate by about 1.1kg/h, when the air flow rate is increased from 479 to 728 kg/h, when the desiccant flow rate is increased from 19.3 to 96.6 kg/h or if the air inlet humidity ratio is increased from 13.6 to 18.6 g/kg for the given reference conditions. The moisture removal rate decreases with increasing air inlet temperature. The dehumidification efficiency increase sharply with increasing desiccant flow rate and slightly increased with air flow rate. It was found also that the dehumidifier efficiency decrease with air inlet temperature and slightly increase with air humidity ratio.

Acknowledgement

The funding provided by DAAD "Deutscher Akademischer Austausch Dienst", German Academic Exchange Service, is gratefully acknowledged.

References

[1] Jaradat, M., Heinzen, R., Jordan, U., Vajen, K., Initial Experiments of a Novel Liquid Desiccant Dehumidifier for Industrial and Comfort Air Conditioning Systems, Proceeding of the 3rd International Conference Solar Air-Conditioning 2009, Palermo (IT), 30.09 - 02.10 2009.

[2] Kathabar technical information, www.kathabar.com, © 2010 Kathabar Systems

[3] M. Krause, W. Saman, K. Vajen, Regenerator Design for Open Cycle Liquid Desiccant Systems - theoretical and Experimental Investigations, Proceedings of the International Conference Solar Air-Conditioning, Staffelstein (DE), 6. - 7.10.2005.

[4] Lowenstein A., Slayzak S., Kozubal E., A Zero Carryover Liquid Desiccant Air Conditioner for Solar Applications, ASME/Solar06, Denver (US).

[5] Lävemann, E. Peltzer, M. ,Solar Air Conditioning of an Office Building in Singapore Using Open Cycle Liquid Desiccant Technology, Proceedings of the International Conference on Solar Air Conditioning, Staffelstein (DE), 06.-07.10.2005.

[6] Jaradat, M., Heinzen, R., Jordan, U., Vajen, K., A Novel Generator Design for a Liquid Desiccant Air Conditioning System, Proceedings of the EuroSun 2008 Conference, Lisbon (PO), 07.10 - 10.10.2008.

[7] Conde, M.R. "Properties of aqueous solutions of lithium and calcium chlorides: formulations for use in air conditioning equipment design", International Journal of Thermal Sciences, vol. 43,pp 367–382.